

Performance Analysis of BTO-Based MZM for 200 Gbps/ λ O-band Intra-Datacenter Interconnects

Weijia Li⁽¹⁾, Felix Eltes⁽²⁾, Essam Berikaa⁽¹⁾, Md Samiul Alam⁽¹⁾, Santiago Bernal⁽¹⁾, Cyriel Minkenberg⁽²⁾
Stefan Abel⁽²⁾, and David V. Plant⁽¹⁾

⁽¹⁾ Department of Electrical and Computer Engineering, McGill University, Montréal, QC H3A 2A7, Canada; weijia.li3@mail.mcgill.ca

⁽²⁾ Lumiphase AG, Laubisrütistrasse 44, 8712 Stäfa, Switzerland

Abstract *This work demonstrates employing a BTO-based silicon photonic MZM for achieving high-speed and long-distance data transmission in the O-band, enabling the transmission of 106 Gbaud PAM4 over a 10 km under the KP4-FEC threshold with a net data rate of 200 Gbps. ©2023 The Author(s)*

Introduction

The growth of bandwidth-hungry applications such as Metaverse, cloud-based services, artificial intelligence applications, and streaming platforms, caused a rapid increase in data traffic. This has led to a strain on the capacity of short-reach datacenter interconnects (DCI), which struggle to keep up with the traffic demand. Specifications for 200 G/ λ are being defined [1], but an increasing emphasis on energy efficiency is fueling demand for low-power modulator technologies.

In this paper we present an empirical study of the performance of an intensity modulated/direct detect (IM/DD), O-band, optical fiber transmission system employing a BTO based silicon photonic MZM. We examine the baud rate (26.5 – 124 Gbaud), PAM order (4, 6, 8), wavelength (1280 – 1330 nm), and reach (0-10 km) trade-offs associated with a BTO-based MZM. This study extends our previous work on a C-band BTO-based MZM to the O-band [2].

BTO Photonic Platform

Our BTO-enhanced photonics platform integrates BTO into an otherwise conventional silicon photonic process flow at wafer-scale. BTO is a transparent, dielectric material that enables low-loss passive components across the O-, C- and L-bands [3-5] as well as active phase shifters with the addition of metal electrodes to create an electric field in the BTO layer. The very strong Pockels effect of BTO enables the design of compact, low-swing, high-speed modulators. In addition, the Pockels effect in BTO can be used to implement ultra-low-power (μ W range) DC phase tuners to control the operating point of the high-speed modulators, offering a reduction by several orders of magnitude compared to thermal phase shifters.

Experimental Setup

Figure 1 illustrates the schematic of the experimental setup. The transmitter generates

PAM symbols from a random bit sequence, and then applies non-linear (NL) compensation based on a lookup table with a 3-symbol memory length. The signal is shaped with a raised-cosine pulse shaping filter at 2 samples per symbol (sps). Subsequently, the signal is re-sampled to 128 GSa/s and filtered using a pre-emphasis digital filter. This filter compensates for the frequency response of the arbitrary waveform generator (AWG), radio frequency (RF) amplifier, and a 20 cm RF cable (1.85 mm connectorized). The digital signal is loaded to the AWG, which drives a 55 GHz SHF 807 RF amplifier. The amplified RF signal is then fed to the MZM through a 67 GHz RF probe.

Optically, we employ a 19 dBm O-band distributed feedback (DFB) laser at 1310 nm wavelength as well as Santec's TSL-570 high-power external cavity laser (ECL) to sweep the operational wavelength. The modulated optical output is transmitted over 0-10 km of standard single-mode fiber (SSMF) and amplified by a Praseodymium-doped fiber amplifier (PDFA) to compensate for the grating coupler insertion loss in the absence of a transimpedance amplifier (TIA) in our receiver. We use a variable optical attenuator (VOA) just before the 70 GHz photodiode (PD) to control the received optical power (ROP). The PD output is then captured by a 256 GSa/s real-time oscilloscope (RTO) for subsequent processing. The receiver DSP operates at 2sps and constitutes of linear feed-forward equalizer (FFE) or polynomial nonlinear equalizer (PNLE). Fig. 1(a) inset shows the optical spectra of a 106 Gbaud PAM4 signal with and without the PDFA, which shows the ASE noise floor added by the optical amplifier.

We at first evaluate the performance of the MZM using a digital communication analyzer with

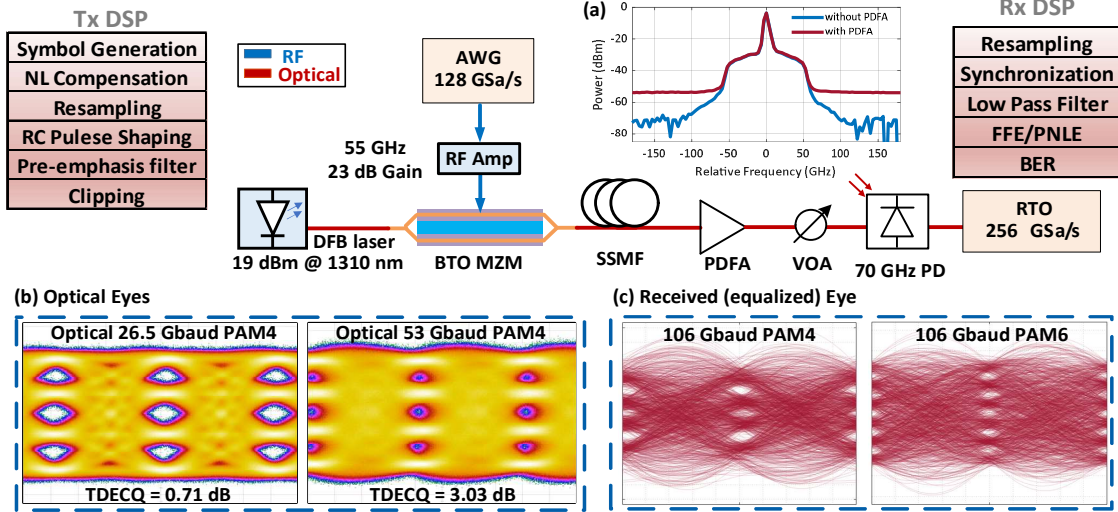


Fig.1: The experimental setup and the DSP routine utilized at the transmitter (Tx) and receiver (Rx). The insert shows: (a) measured optical spectra (at 0.03 nm resolution) of 106-Gbaud PAM-4 signal over 10-km standard single-mode fiber (SSMF) with and without the use of PDFA; (b) optical eye diagrams and TDECQ measurements; (c) The eye diagrams of the equalized 106 Gbaud PAM-4 and PAM-6 signal.

a 120 GHz optical head. The transmitter dispersion eye closure quaternary (TDECQ) [6] is measured after 2 km transmission with 5 linear equalizer taps, as shown in Fig. 1(b). The resulting TDECQ values for 26.5 Gbaud PAM4 (50 Gbps) and 53 Gbaud PAM4 (100 Gbps) are 0.74 dB and 3.03 dB respectively. These measurements indicate that the BTO-based MZM is suitable for use in 100 Gbps applications conforming to the 100GBASE-FR1 IEEE standards [1]. For 106 Gbaud PAM4, the software failed to measure the TDECQ with just 5 taps. Therefore, we processed the 106 Gbaud signals with offline DSP and the recovered eye diagrams are given in Fig. 1(c). 51-tap linear FFE is adopted to generate the eye diagram for 106 Gbaud PAM4, while PNLE with a memory length of 101, 1, and 3 for linear, second and third-order kernels is employed for 106 Gbaud PAM6.

Transmission Performance

Table 1 and Fig. 2 provide a summary of the achieved transmission performance at 1310 nm using the DFB laser. Particularly, Table 1 highlights the potential of BTO-based MZMs for 200 Gbps transmission.

In Fig. 2(a), the BER versus symbol rate is shown for PAM4 signaling after 2 km transmission using linear FFE. To achieve 200 Gbps transmission under the KP4-FEC threshold, 51 FFE taps are required. However,

this high number of taps can be partly attributed to the use of discrete RF components, such as the AWG, RF amplifier, RF cables, and RF probes. The reflections from each of these components create ripples in the combined channel frequency response, and requires a higher number of taps to equalize the received signal. We anticipate that a lower number of taps will suffice for 200 Gbps transmission when using an integrated transceiver.

Figure 2(b) presents the BER performance for various PAM formats transmitted over 2 km (solid line) and 10 km (dashed line). To mitigate non-linearities in higher order PAM formats and to improve the performance, we employed PNLE and achieved successful transmission of 112 Gbaud PAM4 over 2 km while remaining under the KP4-FEC threshold, which provided a 5.8% overhead margin for 200 Gbps/λ transmission. Furthermore, we transmit 100 Gbaud PAM6 and 124 Gbaud PAM4 under the 6.7% overhead HD-FEC BER threshold, corresponding to net data rates of 234 and 232 Gbps, respectively. Adopting a higher SD-FEC threshold, we also transmit 100 Gbaud PAM8 over 10 km under the 20% overhead 2.4×10^{-2} SD-FEC BER threshold, achieving a net data rate of 250 Gbps.

To investigate the transmission performance in the O-band, we utilize a tunable ECL laser with 20 dBm output power and optimize the bias point

Tab. 1: Summary of Net Bitrate Achieved after 10 km Transmission using DFB Laser

BER threshold	FEC overhead	Modulation format	Line-rate (Gbps)	Net bitrate (Gbps)
2.4×10^{-4}	5.8%	106 Gbaud PAM-4	212	200
3.8×10^{-3}	6.7%	124 Gbaud PAM-4 / 100 Gbaud PAM-6	248 / 250	232 / 234
2.4×10^{-2}	20.0%	100 Gbaud PAM-8	300	250

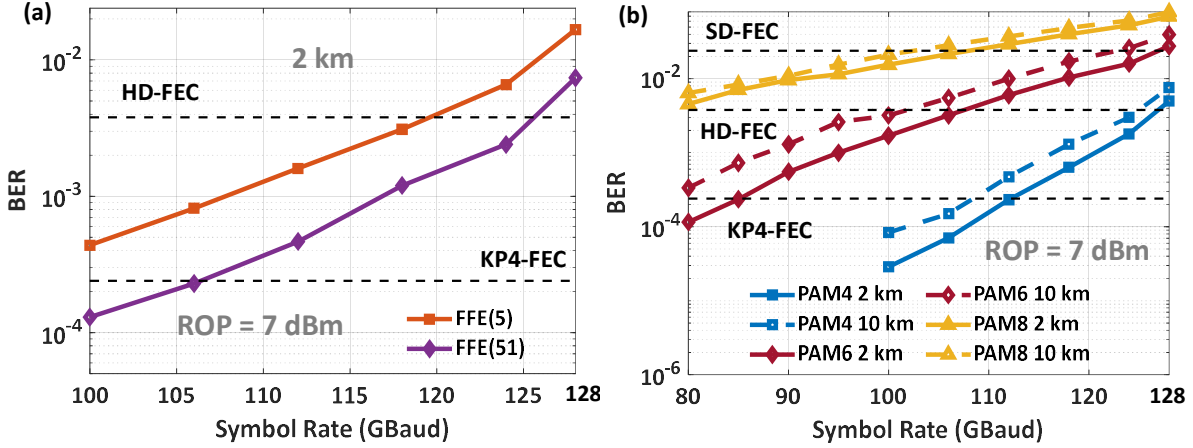


Fig.2: Transmission performance with DFB laser. (a) BER versus symbol rate for PAM-4 over 2 km of SSMF with linear feed forward equalizer (FFE); (b) BER versus symbol rate for different modulation formats with polynomial nonlinear equalizer (PNLE) with a memory length of 101, 1, and 3 for linear, second and third-order kernels.

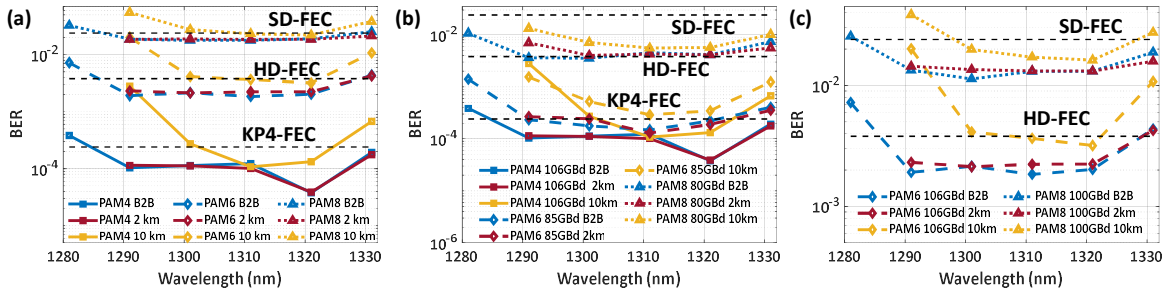


Fig.3: BER performances of different modulation formats with ECL at individual wavelength channels: (a) 106 Gbaud PAM-4, 6, 8; (b) 200 Gbps transmission; (c) 250 Gbps transmission.

for each wavelength as summarized in Fig. 3 and Table 2. Fig. 3(a) plots the BER at 106 Gbaud for the different PAM formats at B2B and after 2 and 10 km transmission across the O-band. Results show that the BER exhibits marginal dependency on wavelength from 1290 to 1320 nm for the considered transmission reach, but considerably increases at the edges of the band due to the narrowband transfer function of the grating coupler, which affects the input into the PDFA and amplifies the increases the contribution of the ASE noise.

Fig. 3(b) studies the BER sensitivity to wavelength considering the different combinations of PAM formats and symbol rates achieving net 200 Gbps. Although 106 Gbaud PAM4 experiences more chromatic dispersion than 85 Gbaud PAM6 at the edge channels after 10 km transmission, our measurements indicate that the PAM4 option still stands as the optimum format for 200 Gbps operation because of its lower SNR and linearity requirements.

Conclusion

Our work demonstrates the potential of O-band BTO-based MZMs for high-speed optical communication systems. We demonstrate net 200 Gbps transmission over 10 km through 1300-

1320 nm, highlighting the promising transmission performance of BTO-based MZMs.

Tab.2: Summary of Net Bitrates with ECL

Length	Net Rate (Gbps)	Modulation Format (Gbaud)	FEC OH	Wavelength range (nm)
10 km	200	106, PAM-4	5.8%	[1301,1321]
		80, PAM-8	20.0%	[1291,1331]
	250	106, PAM-6	6.7%	[1311,1321]
		100, PAM-8	20.0%	[1301,1321]
2 km	200	106, PAM-4	5.8%	[1291,1331]
		85, PAM-6	6.7%	
		80, PAM-8	20.0%	
	250	106, PAM-6	6.7%	[1291,1321]
		100, PAM-8	20.0%	[1291,1331]

Acknowledgements

Work supported by the Swiss State Secretariat for Education, Research, and Innovation under startup accelerator contract MB22.00020.

References

- [1] "IEEE Standard for Ethernet - Amendment 3: Media Access Control Parameters for 50 Gb/s and Physical Layers and Management Parameters for 50 Gb/s, 100 Gb/s, and 200 Gb/s Operation," in IEEE Std 802.3cd-2018 (Amendment to IEEE Std 802.3-2018 as amended by IEEE Std 802.3cb-2018 and IEEE Std 802.3bt-2018) , vol., no., pp.1-401, 14 Feb. 2019, doi: [10.1109/IEEESTD.2019.8649797](https://doi.org/10.1109/IEEESTD.2019.8649797).
- [2] Felix Eltes, Weijia Li, Essam Berikaa, Md Samiul Alam, Santiago Bernal, Cyriel Minkenberg, David V. Plant, and Stefan Abel, "Thin-film BTO-based modulators enabling 200 Gb/s data rates with sub 1 Vpp drive signal," in *Proceedings Optical Fiber Communication Conference (OFC)*, San Diego, CA, USA, 2023, Th4A.2. DOI: [10.1364/OFC.2023.Th4A.2](https://doi.org/10.1364/OFC.2023.Th4A.2)
- [3] Stefan Abel, Felix Eltes, J. Elliott Ortmann, Andreas Messner, Pau Castera, Tino Wagner, Darius Urbonas, Alvaro Rosa, Ana M. Gutierrez, Domenico Tulli, Ping Ma, Benedikt Baeuerle, Arne Josten, Wolfgang Heni, Daniele Caimi, Lukas Czornomaz, Alexander A. Demkov, Juerg Leuthold, Pablo Sanchis and Jean Fompeyrine, "Large Pockels effect in micro- and nanostructured barium titanate integrated on silicon," *Nature Materials* 18(1), 42–47 (2019). DOI: doi.org/10.1038/s41563-018-0208-0
- [4] Felix Eltes, Christian Mai, Daniele Caimi, Marcel Kroh, Yuri Popoff, Georg Winzer, Despoina Petousi, Stefan Lischke, J. Elliott Ortmann, Lukas Czornomaz, Lars Zimmermann, Jean Fompeyrine, and Stefan Abel, "A BaTiO₃-based electro-optic Pockels modulator monolithically integrated on an advanced silicon photonics platform," *Journal of Lightwave Technology* 37(5), 1456–1462 (2019). DOI: [10.1109/JLT.2019.2893500](https://doi.org/10.1109/JLT.2019.2893500)
- [5] Felix Eltes, Daniele Caimi, Florian Fallegger, Marilyne Sousa, Eamon O'Connor, Marta D. Rossell, Bert Offrein, Jean Fompeyrine, and Stefan Abel, "Low-loss BaTiO₃-Si waveguides for nonlinear integrated photonics," *ACS Photonics* 3(9), 1698–1703 (2016). DOI: doi.org/10.1021/acsphotonics.6b00350
- [6] Santiago Echeverri-Chacón, Johan Jacob Mohr, Juan José Vegas Olmos, Piers Dawe, Bjarke Vad Pedersen, Thorkild Franck, Steen Bak Christensen, "Transmitter and Dispersion Eye Closure Quaternary (TDECQ) and Its

Sensitivity to Impairments in PAM4 Waveforms", *Journal of Lightwave Technology* 37(3), 852-860 (2019). DOI: [10.1109/JLT.2018.2881986](https://doi.org/10.1109/JLT.2018.2881986).